Application of regenerated spent bleaching earth as an adsorbent for the carbon dioxide adsorption by gravimetric sorption system

Application of regenerated spent bleaching earth as an adsorbent for the carbon dioxide adsorption by gravimetric sorption system

Melissa Low Phey Phey[1,2], Tuan Amran Tuan Abdullah[1,2,*], Arshad Ahmad[1,2] and Umi Fazara Md Ali[3,4]

[1]Center of Hydrogen Energy, Institute of Future Energy, Universiti Teknologi Malaysia, 81310 Skudai, Johor, Malaysia
[2]School of Chemical and Energy Engineering, Faculty of Engineering, Universiti Teknologi Malaysia, 81310 Skudai, Johor, Malaysia
[3]Chemical Engineering Programme, Faculty of Chemical Engineering Technology, Universiti Malaysia Perlis, Kompleks Pusat Pengajian Jejawi 3, 02600 Arau, Perlis, Malaysia
[4]Centre of Excellence Biomass Utilization (COEBU), Universiti Malaysia Perlis, Kompleks Pusat Pengajian Jejawi 3, 02600 Arau, Perlis, Malaysia

E-mail: tuanamran@utm.my

Abstract. The atmospheric level of carbon dioxide (CO_2) is indicated to be alarming which in turn has contributed to the worldwide environmental issue such as global warming. The goal of this project was to study the adsorption of CO_2 onto regenerated spent bleaching earth (RSBE). Spent bleaching earth (SBE) can be a good adsorbent but it has the weakness in surface area due to the organic impurities left in the pores after being generated from the edible oil processing. Thus, the regeneration processes of SBE by (a) direct heat treatment, and (b) heat treatment followed by nitric acid treatment were studied to enhance the surface area, thus increasing the CO_2 adsorption capacity. The SBE were calcined at four temperatures of 400, 500, 650 and 800 °C in the regeneration process. The surface properties of RSBE were characterized using Thermogravimetric Analysis (TGA), Fourier Transform Infrared (FTIR) analysis and Brunauer–Emmett–Teller (BET) surface area analysis. The CO_2 adsorption capacity on RSBE produced by heat treatment followed by nitric acid treatment was shown to be more effective than RSBE produced by direct heat treatment. RSBE_500_HNO3 offered highest surface area (192.81 m^2/g) and give highest CO_2 adsorption capacity of 86.67 mg CO_2/g. In comparison to the low pressure condition, the high pressure CO_2 adsorption values recorded for both RSBE were significantly better.

1. Introduction

The global warming rate has accelerated dramatically over the centuries. As greenhouse gas (GHG) emissions blanket to the Earth continues to rise and this leads to the greenhouse effect which occurs once the atmosphere is absorbing the infrared radiation is then emitted from the surface toward the space. Carbon dioxide (CO_2) is deemed as the principal trace gas that caused greenhouse effect. A continuous increase in the atmospheric concentrations of CO_2 have caused negative effects to the

environment so do on the living organisms. In fact, this has inevitably aroused great concern of the public on enormous and the impact of uncontrolled emission of CO_2 towards the environment and climate change. By contrast, the endeavour of reversing this upward tendency becomes more difficult. According to the analysis and prediction of Intergovernmental Panel on Climate Change (IPCC), the global atmospheric CO_2 concentration may rise to 570 ppm of CO_2 by the year of 2100 if effective and proper measures are not carried out. This situation causes an average increment of global temperature by 1.9°C and an average increment of sea level by 3.8 m [1]. As a result, international cooperation has been put on the agenda in the process of reducing CO_2 emission and mitigation has been approached expressly from the perspective of long term development sustainability development [2].

In order to reduce and control the atmospheric CO_2 level, several practicable actions can be taken into consideration, for example, substituting carbon emitting fuel with non-carbon emitting fuel enhances the combustion efficiency, eliminating the utilization of fossil fuel by employing the Carbon Capture Sequestration (CCS) technology. CCS provides a lower cost means to capture CO_2 from the power station and industrial CO_2 containing stream followed by transportation and storage of the compressed CO_2 [3]. As a result, CCS is considered as an effective CO_2 abatement technology. Adsorption, cryogenic separation, membrane separation, and chemical separation technique are some of the CO_2 capture technologies that have been used [3]. Adsorption has been established to be the superior CO_2 capture technique due to its low capital and operational costs, simplicity of design, low energy requirements, and lower secondary wastes generation [4].

Several adsorbents have been employed in the adsorption process, such as clay, activated carbon (AC), activated alumina, granular ferric hydroxide and zeolite. Throughout this research, clay was selected as CO_2 adsorbent because of its several advantages such as high availability and stability. In this context, clay is considered a natural material for CO_2 adsorption. A form of clay with a montmorillonite structure, such as bentonite, is referred to as bleaching earth (BE) in the world of commercial. BE is a naturally mineral-rich clay that has been acid-treated. It mostly comprises silica, followed by aluminum, and a smaller amount of other cations like iron, magnesium, and calcium. In the refining process of crude palm oil, BE is used as an adsorbent for removing the colouring matters, metals, oxidized materials, phospholipids, and undesirable residues [5]–[7].

SBE or spent clay is categorized as solid wastes, generating from the pre-treatment of crude palm oil (CPO) in an edible oil refinery [7]–[10]. It is also an alumino-silicate mineral that mainly consists of montmorillonites with a 2:1 unit layer structure [11]. Usually, SBE has an unpleasant odour, consisting of residual oil and clay minerals [12]. SBE normally still contains 20 – 40% residual oil by weight, depending on the activity of the bleaching [9], [13]. The oxidation of the residual oil in the earth to the point of spontaneous auto-ignition will cause fire and pollution hazards because of the autocatalysis action of clay minerals and association of GHG emissions upon the disposal of SBE [7]–[9], [14]. So, its disposal procedure poses an acute storage and management problem.

Consequentially, it is critical in developing new cost-effective SBE disposal and usage methods as soon as possible to ensure the ecosystem's long-term viability. Due to its availability, low cost, and physical and chemical features, such as high ion exchange capacity, high surface area, and chemical and mechanical stability, SBE has been used in a variety of applications. RSBE is widely employed in adsorption field, including decolourization, refinement of edible oils, fillers, desiccants, adsorbents, wastewater treatment, medical science, catalysis and others [15]–[20]. Unfortunately, there has been limited exploration on CO_2 capture via adsorption on RSBE. In order to increase their adsorption capacities, RSBE was chosen to study in this research. According to Kaye et al., the gas adsorption capacity was significantly influenced by the preparation and handling procedures of the porous samples [21].

According to Pranowo et al., the regeneration of SBE was carried out by acid treatment followed by thermal treatment [17]. They mention that using acid to regenerate SBE can enhance its absorption capacity. Furthermore, two regeneration methods carried out by Wafti et al. show that the direct heat treatment was more efficient as compare to solvent extraction followed by heat treatment [20]. Majid and Mat found that impregnating SBE using sulphuric acid followed by heat treatment results in a highly

efficient performance in the decolourization of palm oil mill final effluent discharge. From the research of Tang et al., the calcination temperature of SBE is a critical aspect in the thermal regeneration process for removing heavy metal ions in wastewater [18].

The purpose of this research was to determine the possibility of using RSBE for CO_2 adsorption. To the best of my knowledge, CO_2 capture via adsorption on RSBE is limited exploration. Thermally treated and surface modified clays (acidic activation) were used to improve the surface area feature as well as to improve the adsorption capacity of the RSBE. Surface characterization and CO_2 adsorption experiments on different regeneration processes of SBE were performed by a gravimetric sorption system to study the adsorption behaviour of these materials.

2. Experimental

2.1. Materials

Spent bleaching earth (SBE) was obtained from palm oil refinery (Sime Darby Sdn. Bhd.), Pasir Gudang, Johor, Malaysia. The nitric acid (HNO_3) (purity = 65%) was purchased from RCl Labscan.

2.2. Regeneration process of SBE

SBE was regenerated by direct heat treatment in the air atmosphere at 4 different temperatures of 400 °C, 500 °C, 650 °C and 800 °C for 2 h. Another 4 samples were calcined at 400 °C, 500 °C, 650 °C and 800 °C for 2 h, followed by impregnated with nitric acid (1 M). A 1:5 ratio of SBE and nitric acid (w/v) was applied in the acid treatment process. A magnetic stirrer was used to agitate the SBE mixture with nitric acid for 2 h at 80 °C. After that, SBE was filtered and rinsed multiple times till pH 7 to remove the acid by using distilled water. The RSBE was used as an adsorbent in the CO_2 adsorption experiment after 24 h drying in an oven at 105 °C for. The adsorbents were marked as SBE: untreated Spent Bleaching Earth, RSBE_400: SBE regenerated at 400 °C, RSBE_500: SBE regenerated at 500 °C, RSBE_650: SBE regenerated at 650 °C, RSBE_800: SBE regenerated at 800 °C, RSBE_400_HNO3: SBE regenerated at 400 °C followed by nitric acid treatment, RSBE_500_HNO3: SBE regenerated at 500 °C followed by nitric acid treatment, RSBE_650_HNO3: SBE regenerated at 650 °C followed by nitric acid treatment, RSBE_800_HNO3: SBE regenerated at 800 °C followed by nitric acid treatment, corresponding to the above regenerated conditions, respectively.

2.3. Characterization methods

2.3.1. Thermogravimetric analysis. Thermogravimetric analysis (TGA) was performed on a Shimadzu TGA-50. During the data collection, the air was flowed through the apparatus at a rate of 20 mL/min. The sample temperature was ramped at 10 °C/min from 30 to 800 °C to determine the weight loss and thermal decomposition of samples

2.3.2. Fourier transform infrared spectroscopy analysis. Fourier transform infrared (FTIR) spectra were collected over the range 400–4000 cm^{-1} using a SHIMADZU IRPrestige-21 IRAffinity-1 FTIR-8400S to determine the functional groups on the RSBE structure. The difference spectrum was created by subtracting a KBr backdrop from the sample scan.

2.3.3. Surface area analysis. The single point specific surface area of the samples was analysed using Micromeritics FlowSorb III 2310 surface area analyser by a continuous flow of a 30% N_2/70% Helium gas mixture over the sample at atmospheric pressure. The samples were degassed for 30 mins at 200 °C at first for eliminating all gases and moisture adsorbed from the atmosphere. The Brunauer−Emmett−Teller (BET) method was used to calculate the specific surface area.

2.4. CO_2 adsorption test

The CO_2 adsorption capacity of the samples was determined using Rubotherm-TA instrument's gravimetric sorption analyser isoSORP®. The gravimetric sorption analyser's sample container was filled with 10 mg of RSBE. Pre-treatment was carried out to reduce the adsorbed moisture by heating the RSBE to 100 ° C under vacuum for 2 h before the adsorption. The buoyancy mode was applied to acquire precise substrate's volume and weight for proper adsorption weight. Buoyancy was tested at 30 °C with a helium (He) gas at a flow rate of 500 mL/min and a pressure range of 0 to 30 bars. At 30 °C and pressure varying from 0 to 30 bars, pure CO_2 (500 mL/min) was employed in the adsorption test.

3. Results and discussions

3.1. Characterization of SBE and RSBE

3.1.1. Thermogravimetric analysis. Thermogravimetric analysis (TGA) was used to evaluate the thermal behaviour of SBE and RSBE at temperatures range from 30 to 800 °C in synthetic air. Figure 1 shows the weight loss curves for untreated and RSBE. As seen in the TGA profile, the weight loss of the sample, which is categorized into multiple thermal degradation processes, having different weight loss percentage by manipulating the calcination temperature. The weight loss is observed and categorized into 4 stages as listed in Table 1.

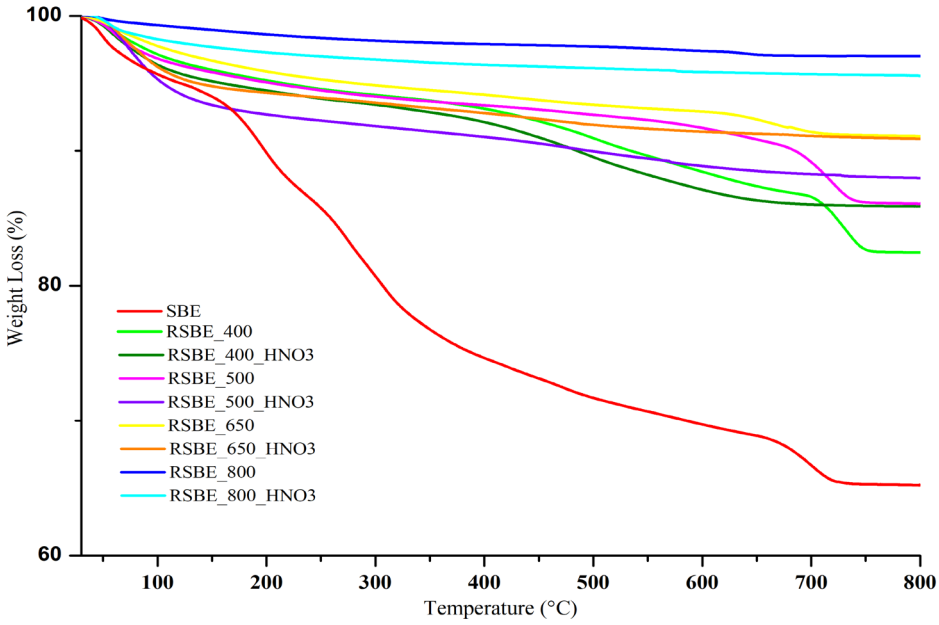

Figure 1. TGA profile of SBE and RSBE samples.

Untreated SBE had a weight loss of 25.4% at 400 °C, 28.3% at 500 °C, 31.1% at 650 °C and 34.7% at 800 °C, as illustrated in Figure 1. The first weight loss of 5.97% that occurred below 150 °C can be ascribed to the thermal dehydration of trapped water molecules on the surface of materials [22]. The elimination of a majority of the coordinated water and decomposition of organic material (evaporation of volatile matter) from the SBE resulted in a quick decline in the sample weight of 17.26% at the second dehydration phase from 150 to 350 °C [13], [22], [23]. Weight loss in the third and fourth steps, which occur at 350–650 °C (7.9%) and over 650 °C (3.6%), were linked to the burning of leftover oils from SBE and the loss of structural hydroxyl groups in silica (Si-OH) bonding, which is well recognized as a result of OH groups releasing from various places within the montmorillonite structure [13], [22]–[24]. A previous study by Al-Zahrani and Daous found that the calcination of SBE causes the combustion of organic compounds, colour pigments, and oil adsorbed on the surface or trapped in the voids of the spent

clay [15]. Aside from that, the OH-O link between the clay layers will be broken, and the crystal structure of the clay may be altered as a result of dehydration.

In the regeneration temperature range of 400 to 800 °C, 17.5% weight loss was reported for RSBE_400, 13.9% for RSBE_500, 8.9% for RSBE_650 and 4.45% for RSBE_800 after heat treatment. As seen in Figure 1, the higher the calcination temperature, the smaller the weight loss. Below 150 °C, the TGA curves of RSBE_400, RSBE_500, RSBE_650 and RSBE_800 exhibited a weight loss of about 4.0%, 4.2%, 3.3% and 2.0%, respectively, due to the dehydration of the surface water molecules that might be happened during the storage of the adsorbent [25]. From Figure 1 (RSBE_400, RSBE_500 and RSBE_650), the second weight loss phase (150–400 °C) approaches a linear profile with weight loss of 2.9%, 2.4%, and 2.5%, respectively. However, in the third phase (400–650 °C), RSBE_400 shows a drastic weight loss of about 5.7% when compared to RSBE_500 (2.5%) and RSBE_650 (1.9%), indicating that the interlayer water was not entirely eliminated by the adsorbent's calcination at 400 °C [25]. In the fourth phase, RSBE_400, RSBE_500 and RSBE_650 lose weight at nearly identical rates of 4.9%, 4.8% and 4.3%, respectively. The weight loss above phase two (400–800 °C) can be assigned to the release of structural water and the oxidation of a small amount of organic matter from residual impurities under an air atmosphere [22]. The number of organic impurities adhered to the SBE regenerated at 800 °C (RSBE_800) was smaller than that of 400 °C (RSBE_400), 500 °C (RSBE_500) and 600 °C (RSBE_650), which attributed to the least weight loss occurred for RSBE_800 at second (1.4%), third (0.8%) and fourth weight loss phase (0.1%) as compared to RSBE_400, RSBE_500 and RSBE_650.

Weight loss for SBE regenerated by heat treatment followed by nitric acid treatment in the temperature range was about 14.1% (RSBE_400_HNO3), 12% (RSBE_500_HNO3), 9.1% (RSBE_650_HNO3), and 3% (RSBE_800_HNO3), respectively. The weight loss of RSBE 400 and RSBE 500 is greater than that of RSBE 400_HNO3 and RSBE_500_HNO3 by 3.4% and 1.9%, indicating that the organic impurities do not entirely decompose below 500 °C calcination temperature. Similar TGA profiles were recorded for RSBE_650 and RSBE_650_HNO3, which approaches a linear profile with different weight loss of only 0.2% and almost similar TGA profiles for RSBE_800 and RSBE_800_HNO3, which approaches a linear profile with different weight loss of only 1.45%. Hence, calcining SBE at 650 °C and 800 °C is sufficient to eliminate the impurities and oil.

Table 1. Weight loss of SBE and RSBE by TGA.

Sample	**Weight loss (%)**				**Overall weight loss (%)**
	< 150 °C	**150 – 350 °C**	**350 – 650 °C**	**> 650 °C**	
SBE	5.97	17.26	7.9	3.6	34.7
Sample	**< 150 °C**	**150 – 400 °C**	**400 – 650 °C**	**> 650 °C**	**Overall weight loss (%)**
RSBE_400	4.0	2.9	5.7	4.9	17.5
RSBE_400_HNO3	3.8	4.1	5.8	0.4	14.1
RSBE_500	4.2	2.4	2.6	4.7	13.9
RSBE_500_HNO3	6.6	2.4	2.5	0.5	12
RSBE_650	3.3	2.5	1.9	1.2	8.9
RSBE_650_HNO3	5.3	1.9	1.5	0.4	9.1
RSBE_800	1.0	1.1	0.8	0.1	3
RSBE_800_HNO3	2.3	1.3	0.6	0.2	4.4

TGA analysis shows that as the temperature increases, the weight loss of the samples decreases, indicating that the organic matter content of RSBE gradually decreases. Thus, the results demonstrate that when SBE is calcined at a higher temperature, the removal of organic impurities is higher than SBE calcined at lower temperature. The weight losses at this stage were clearly higher for SBE regenerated

by direct heat treatment than for SBE regenerated by heat and nitric acid treatment, indicating that SBE regenerated by direct heat treatment included more organic matter.

3.1.2. Fourier transform infrared spectroscopy analysis. Fourier transform infrared (FTIR) spectroscopy is used to investigate the functional groups on the untreated SBE and treated SBE. Figure 2 shows the FTIR spectra of untreated SBE and RSBE calcined at different calcination temperatures (400, 500, 650 and 800 °C), as well as four samples that were impregnated by nitric acid following heat treatment within region 400–4000 cm^{-1}.

Both the untreated SBE and treated SBE have similar spectra at 1034, 1042, 1049, 1057, 1072 and 1080 cm^{-1}, which are attributed to the presence of silicate matrix (Si-O-Si stretching vibrations), 795 cm^{-1} attributed to the presence of silica/quartz impurities (Si-O vibrations), and 463, 470 and 478 cm^{-1} attributed to the Si-O-Al vibrations [13], [22], [26]. The fact that SBE and RSBE had identical spectra implies that heat remediation followed by acid impregnating has no effect on the structure of bleaching earth montmorillonite [26], [27]. After being treated with nitric acid, the intensity peak in the region 1034–1080 increased because nitric acid treatment suggests an increase in amorphous silica content owning to partial destruction of the tetrahedral sheet, which is corroborated by the study of Krupskaya et al. [28]. They mention that the Si content in powder samples increased after the nitric acid treatment. In addition, the adsorption band of the O−H stretching and bending vibrations at 1628, 1635, 1643 cm^{-1} also confirms the existence of interlayer water inside the montmorillonite matrix. The intensities of these bands become weaker after the regeneration process, indicating that the adsorbed water and the hydroxyl groups have been removed [13], [18].

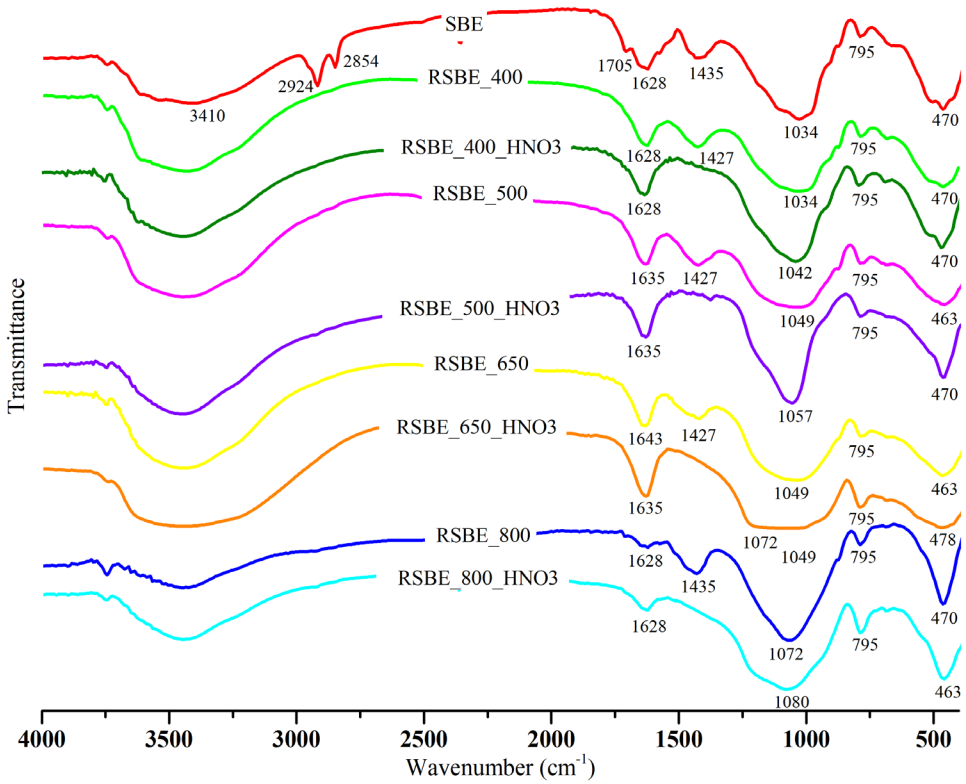

Figure 2. FTIR spectra of SBE and RSBE samples.

The FTIR spectrum of SBE exhibited characteristic absorption bands at 3410 cm^{-1} which was related to the interlayer water adsorption and structural hydroxyl group stretching vibrations. The disappearance of this band followed by the regeneration process of SBE was resulted from the elimination of adsorbed water and hydroxyl groups [18]. The contribution of C−H stretching vibration of $–CH_3$, $–CH_2–$ and C−H

is represented by wavenumbers 2924 and 2854 cm^{-1} [18]. These absorption bands disappear after the regeneration of SBE, indicating a change in the chemical composition of RSBE by the conversion or decomposition of organic impurities for both direct heat treatment process and heat treatment followed by acid treatment process [18]. Furthermore, by presenting the carboxyl groups (C=O stretching vibration), the absorption band at 1705 cm^{-1} reveals the characteristics of organic residual oil bands. After SBE is regenerated, the absorption band at 1705 cm^{-1} disappears, implying that this alternation may affect the adsorption capacity of RSBE [18]. The absorption band at wavenumbers 1427 and 1435 in SBE, RSBE_400, RSBE_500, RSBE_650 and RSBE_800 was attributed mostly to the stretching vibration of C=C, correlating to the existence of organic matter in untreated SBE and SBE regenerated by direct heat treatment [22]. In RSBE_400_HNO3, RSBE_500_HNO3, RSBE_650_HNO3 and RSBE_800_HNO3, the absorption bands disappear, which implies that the thermal remediation followed by acid treatment, in reality, eliminate the organic adsorbed residues in the pores.

3.1.3. Surface area analysis. The results of the specific surface area of untreated SBE and RSBE are presented in Table 2.

Table 2. BET surface areas of SBE and RSBE.

Sample	Surface Area (m^2/g)
SBE	13.40
RSBE_400	74.14
RSBE_400_HNO3	146.31
RSBE_500	92.43
RSBE_500_HNO3	192.81
RSBE_650	80.22
RSBE_650_HNO3	181.79
RSBE_800	13.05
RSBE_800_HNO3	48.27

The pores in SBE may be contaminated with the organic impurities, resulting in a smaller specific surface area (13.40 m^2/g). In contrast, the specific surface area of RSBE increases noticeably in the temperature of regeneration process range from 400−500 °C, decreases slightly at calcination temperature of 650 °C and then decreases obviously with additional calcination temperature increases up to 800 °C. The elimination of coordinated water or hydroxyl structural water, the decomposition of the organic matter and the structure change of SBE regenerated at different calcination temperatures may related to the above results [18]. The elimination of water below 650 °C results in an increase in the sample's specific surface area, which leads to an improvement in the adsorption properties. The lowest specific surface area (13.05 m^2/g) were obtained in RSBE_800. SBE regenerated by heat treatment at highest temperatures of 800 °C may cause the pore collapse and structural damage, resulting in a decrease in specific surface area [20]. The decrease in surface area found for RSBE_650 and RSBE_800 could be due to this structural modification. The current findings appear to be consistent with the research of Wafti et al., who discovered that the specific surface area of the RSBE was maximal at 500 °C calcination temperature, whereas the lowest specific surface area was found in SBE regenerated at 800 °C regeneration temperature [20].

RSBE produced by heat treatment followed by nitric acid treatment (RSBE_400_HNO3, RSBE_500_HNO3 and RSBE_650_HNO3 and RSBE_800_HNO3) has a greater surface area than RSBE produced by direct heat treatment (RSBE_400, RSBE_500, RSBE_650, and RSBE_800). The highest surface area (192.81 m^2/g) was observed for the RSBE_500_HNO3. According to Tsai et al. 2002, impregnating with acid is known to remove carbon residues and water-soluble components from the SBE after being calcined [13]. As a result, the final products obtained after heat and acid treatment should theoretically yield pores with well-developed structure.

While analysing the adsorption and desorption isotherms of N_2 to determine the surface area, carbon residues remaining in the adsorbents may be blocking pore entrances to the N_2 molecules, resulting in small surface areas of the RSBE produced by direct heat treatment [13]. The FTIR analysis can reveal the impact of acid treatment on the chemical properties (Figure 2). It is clear that direct heat regeneration could not entirely eliminate the residues in the pores.

3.2. CO_2 adsorption analysis

The adsorption capacity of CO_2 on adsorbents RSBE under a different pressure up to 30 bar at a constant temperature of 30 °C are shown in Figure 3. The highest CO_2 adsorption capacity of 86.67 mg CO_2/g was observed on RSBE_500_HNO3 at 30 bar, which was higher than those of RSBE_400 at 49.08 mg CO_2/g, RSBE_400_HNO3 at 74.41 mg CO_2/g, RSBE_500 at 53.06 mg CO_2/g, RSBE_650 at 52.22 mg CO_2/g, RSBE_650_HNO3 at 80.16 mg CO_2/g, RSBE_800 at 10.35 mg CO_2/g and RSBE_800_HNO3 at 24.72 mg CO_2/g. From the results of adsorption experiments, CO_2 adsorption capacity on the RSBE adsorbents increase with increasing pressure.

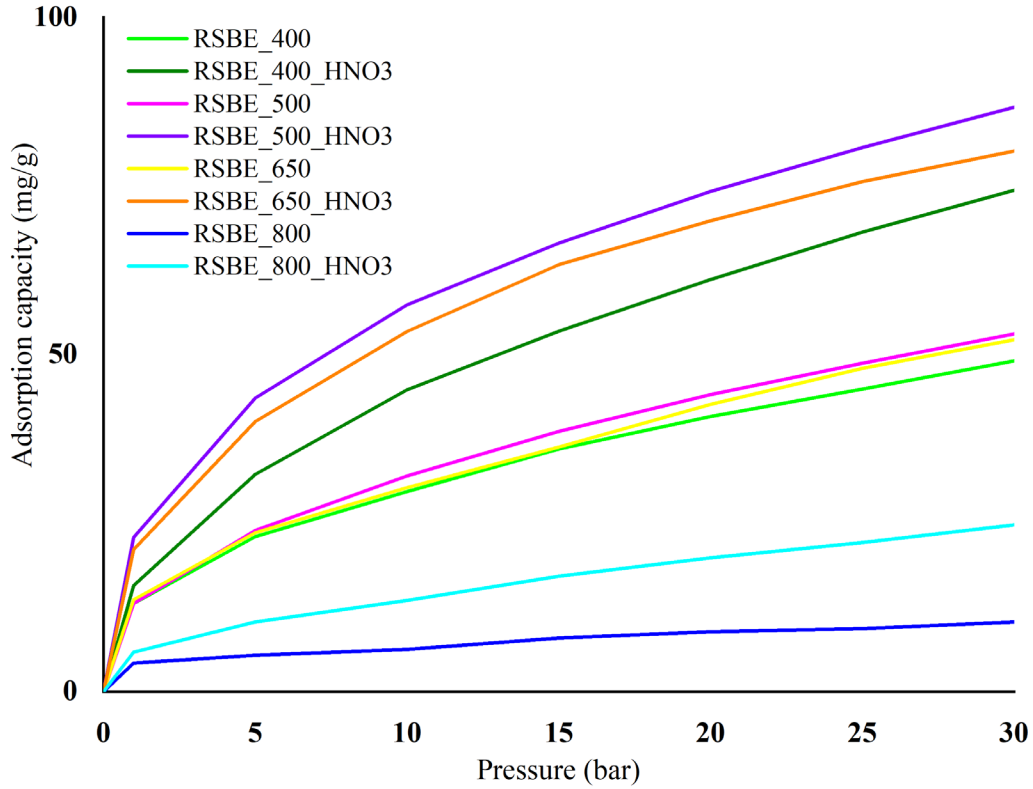

Figure 3. Effect of the regeneration process of SBE on CO_2 adsorption capacity.

The temperature of the heat treatment during the regeneration process of SBE is a critical factor in determining the CO_2 adsorption capacity on RSBE. The adsorption capacity increases slightly on the SBE calcined in the temperature range from 400 to 500 °C at high pressure of 30 bar. However, the adsorption capacity started to decrease on SBE calcined in the temperature range from 500 to 650 °C of around 0.84 mg CO_2/g. After that, SBE regenerated in the temperature range from 650 to 800 °C shows a significant drop of roughly 41.87 mg CO_2/g. The lowest CO_2 adsorption capacity was observed in RSBE_800 because of its poor surface area as a result of the high calcination temperature at 800 °C. The unfilled pores of RSBE provide area for CO_2 adsorbate to be captured. However, high calcination temperature can lead the structural damage and pore collapse, resulting in a reduction in specific surface area and hence less area for capturing adsorbate of CO_2 [20].

SBE was impregnated with nitric acid after the heat treatment to remove its carbon residues and water-soluble components for improving the adsorption capacity. The elimination of organic impurities after nitric acid treatment was revealed by FTIR analysis. This also accords with the current observations from Pranowo, which showed that the pale soil becomes negatively charged after the dissolution of Al^{3+} ions and other metal ions from the pale soil lattice layer through a cation exchange of mineral salts (Ca^{2+} and Mg^{2+}) in the bleaching earth interlayer with H^{+} ions from acid during the acid treatment [17]. As a result, the surface area of RSBE was increased, yielding pores with a well-developed structure. Thereby, the adsorption capacity also increased. RSBE_500_HNO3 had the maximum adsorption capacity because of its highest surface area, which allowed more CO_2 molecules to bind to its active sites [29]. From this study, RSBE produced by heat treatment followed by nitric acid treatment has a better adsorption capacity than RSBE produced by direct heat treatment.

Previous experimental studies from Stanly et al. mention that the CO_2 adsorption of clay depends on the surface area, especially the internal pore volume [30]. The current findings seem to be consistent with those of Zulkurnia et al., who found that the maximum adsorption capacity was observed in the adsorbents with highest surface area [29]. Other important findings from Dinda showed that a decrease in CO_2 adsorption capacity on the adsorbent might be related to a decrease in effective surface area and active sites for CO_2 adsorption [2]. The results of this study indicate that the adsorption capacity of an adsorbent is related to its own surface functional groups and specific surface area which determines the final adsorption outcomes.

Comparison of the CO_2 adsorption capacity of a several adsorbents can be seen in Table 3. The better performance attained in the adsorbent with higher surface area can be found in the activated carbon and zeolite, demonstrating that surface area plays a key role in CO_2 adsorption performance. However, the performance of CO_2 adsorption is also influenced by the treatment technique and material used as adsorbent. Chitosan clay can be one of the promising adsorbent in CO_2 adsorption as shown in Table 3 due to the high CO_2 uptake with only 71.26 m^2/g of surface area. From the comparison table, we can know that the regenerated spent bleaching earth can be one of the promising adsorbent in the CO_2 capture and utilization. Further improvement can be made in future to improve its CO_2 adsorption capacity.

Table 3. Comparison of the adsorption capacity of adsorbents for CO_2 adsorption.

Adsorbent	Surface area (m^2/g)	Performance (mg CO_2/g)	Ref.
Activated carbon (AC)			
Chemically Modified AC With Nitric Acid and Ammonium Aqueous	634–865	205–333	[31]
AC prepared with olive trees	602	109.50	[32]
Activated Alumina			
Diethanolamine activated alumina beads	207	55.94	[33]
Piperazine-modified activated alumina	90.7	222.01	[34]
Granular ferric hydroxide			
Sodium hydroxide-modified granular	378.23	27.10	[35]
Zeolite			
13X zeolites	698	330	[36]
5A zeolites	560	280	
Clay			
Chitosan bleaching earth	71.26	344.98	[37]
Amine-functionalized clays	107–274	14–40.7	[38]
Present study (RSBE)	192.8	86.67	-

4. Conclusions

The aim of this research was to study the regeneration process of SBE through two regeneration methods, direct heat treatment and heat treatment followed by nitric acid treatment towards CO_2 adsorption capacity. From the CO_2 adsorption experiment, SBE regenerated by heat treatment followed

by nitric acid treatment was shown to be more effective than direct heat treatment at high pressure of 30 bar. In addition, the nitric acid treatment has a significant impact on the surface area as well as the functional structure of the final samples. In summary, RSBE calcined at 500 °C followed by nitric acid treatment have the most promising potential for the CO_2 adsorption with the adsorption capacity of 86.67 mg CO_2/g which was due to the largest surface area of 192.81 m^2/g obtained. Thus, RSBE produced by heat treatment followed by nitric acid treatment displays an excellent adsorption performance for CO_2 adsorption. This research will serve as a base for future studies and can be applied to a wide-scale industry due to its green and straightforward method, low toxicity, cheap cost and high efficiency of the clay adsorbent prepared from SBE.

Acknowledgements
The authors acknowledged the financial support from Malaysia-Thailand Joint Authority (MTJA) Research Grant (Vote. No. R.J130000.7609.4C172) and Collaborative Research Grant (CRG/UniMAP/9023-00023).

References
[1] V. [Masson-Delmotte *et al.*, "IPCC: Climate Change 2021: The Physical Science Basis," *Cambridge Univ. Press. Press.*, p. 42, 2021.
[2] Dinda S. 2013 Development of solid adsorbent for carbon dioxide capture from flue gas *Sep Purif Technol* **109** 64-71.
[3] Krishnaiah D, Bono A, Anisuzzama S, Joseph C, Khee T. 2014 Carbon Dioxide Removal by Adsorption *Journal of Applied Sciences* **14**(23) 3142–3148.
[4] Songolzadeh M, Soleimani M, Takht Ravanchi M, Songolzadeh R. 2014 Carbon dioxide separation from flue gases: a technological review emphasizing reduction in greenhouse gas emissions *Scientific World Journal* **2014** 828131.
[5] Bakhtiari AR, Zakaria MP, Yaziz MI, Lajis MNHL, Bi X. 2014 Environment Asia *Environment Asia* **7**(1) 104–111.
[6] Beshara A, Cheeseman CR. 2014 Reuse of spent bleaching earth by polymerisation of residual organics *Waste Manage (Oxford)* **34**(10) 1770-4.
[7] Marrakchi F, Bouaziz M, Hameed BH. 2017 Activated carbon–clay composite as an effective adsorbent from the spent bleaching sorbent of olive pomace oil: Process optimization and adsorption of acid blue 29 and methylene blue *Chem Eng Res Des* **128** 221-30.
[8] Cheong KY, Loh SK, Salimon J. 2013 Effect of spent bleaching earth based bio organic fertilizer on growth, yield and quality of eggplants under field condition *AIP Conference Proceedings* **1571**(1) 744-8.
[9] Loh SK, Cheng SF, May C, Ngan M. 2006 A Study of Residual Oils Recovered from Spent Bleaching Earth: Their Characteristics and Applications *American Journal of Applied Sciences* **3**(10) 2063–2067.
[10] Suhartini S, Hidayat N, Wijaya S. 2011 Physical properties characterization of fuel briquette made from spent bleaching earth *Biomass Bioenergy* **35**(10) 4209-14.
[11] Loh SK, Cheong K, Choo Y, salimon J. 2015 Formulation and optimisation of spent bleaching earth-based bio organic fertiliser *Journal of oil palm research* **27**(1) 57-66.
[12] B. Mu 2018 Regeneration and recycling of spent bleaching earth in *Handbook of Ecomaterials*.
[13] Tsai WT, Chen HP, Hsieh MF, Sun HF, Chien SF. 2002 Regeneration of spent bleaching earth by pyrolysis in a rotary furnace *J Anal Appl Pyrolysis* **63**(1) 157-70.
[14] Su C, Duan L, Donat F, Anthony EJ. 2018 From waste to high value utilization of spent bleaching clay in synthesizing high-performance calcium-based sorbent for CO2 capture *Applied Energy* **210** 117-26.
[15] Al-Zahrani AA, Daous MA. 2000 Recycling of Spent Bleaching Clay and Oil Recovery *Process Safety and Environmental Protection* **78**(3) 224-8.
[16] Boukerroui A, Ouali M-S. 2000 Regeneration of a spent bleaching earth and its reuse in the refining

of edible oil *J Chem Technol Biotechnol* **75** 773-6.
[17] Pranowo D, Dewanti BsD, Fatimah H, Setyawan H. 2020 Optimization of regeneration process of spent bleaching earth *IOP Conference Series: Earth and Environmental Science* **524** 012011.
[18] Tang J, Mu B, Zheng M, Wang A. 2015 One-Step Calcination of the Spent Bleaching Earth for the Efficient Removal of Heavy Metal Ions *ACS Sustainable Chemistry & Engineering* **3**(6) 1125-35.
[19] Tian H, Shao Y, Zhang L, Jia P, Zhang Z, Liu Q, et al. 2020 Clay as support for copper catalysts for the hydrogenation of furfural and phenolics *Journal of Chemical Technology & Biotechnology* **95**(5) 1400-11.
[20] Sulihatimarsyila N, Abd Wafti NS, Cheah, Yoo K, Lin S, Lin, et al. 2011 Regeneration and characterization of spent bleaching clay *Journal of oil palm research* **23** 999-1004.
[21] Kaye SS, Dailly A, Yaghi OM, Long JR. 2007 Impact of preparation and handling on the hydrogen storage properties of Zn4O(1,4-benzenedicarboxylate)3 (MOF-5) *J Am Chem Soc* **129**(46) 14176-7.
[22] Liang X, Yang C, Su X, Xue X. 2020 Regeneration of spent bleaching clay by ultrasonic irradiation and its application in methylene blue adsorption *Clay Minerals* **55**(1) 24-30.
[23] Sapawe N, Hanafi MF. 2018 Analysis of the pyrolysis products from spent bleaching clay *Materials Today: Proceedings* **5**(10, Part 2) 21940-7.
[24] Naser J, Avbenake OP, Dabai FN, Jibril BY. 2021 Regeneration of spent bleaching earth and conversion of recovered oil to biodiesel *Waste Manage (Oxford)* **126** 258-65.
[25] Pongstabodee S, Pornaroontham P, Pintuyothin N, Pootrakulchote N, Thouchprasitchai N. 2016 CO2 capture performance of bi-functional activated bleaching earth modified with basic-alcoholic solution and functionalization with monoethanolamine: isotherms, kinetics and thermodynamics *Journal of Environmental Sciences* **48** 126-37.
[26] Sabour MR, Shahi M 2018 Spent Bleaching Earth Recovery of Used Motor-Oil Refinery *Civ. Eng. J.* **4**(3) 572.
[27] Invernizzi C, Daveri A, Vagnini M, Malagodi M. 2017 Non-invasive identification of organic materials in historical stringed musical instruments by reflection infrared spectroscopy: a methodological approach *Anal Bioanal Chem* **409**(13) 3281-8.
[28] Krupskaya VV, Zakusin SV, Tyupina EA, Dorzhieva OV, Zhukhlistov AP, Belousov PE, et al. 2017 Experimental Study of Montmorillonite Structure and Transformation of Its Properties under Treatment with Inorganic Acid Solutions *Minerals* **7**(4) 1–15.
[29] Zulkurnai NZ, Md. Ali UF, Ibrahim N, Abdul Manan NS. 2017 Carbon Dioxide (CO2) Adsorption by Activated Carbon Functionalized with Deep Eutectic Solvent (DES) *IOP Conference Series: Materials Science and Engineering* **206** 012001.
[30] Stanly S, Jelmy EJ, Nair CPR, John H. 2019 Carbon dioxide adsorption studies on modified montmorillonite clay/reduced graphene oxide hybrids at low pressure *J Environ Chem Eng* **7**(5) 103344.
[31] Giraldo L, Vargas DP, Moreno-Piraján JC. 2020 Study of CO2 Adsorption on Chemically Modified Activated Carbon With Nitric Acid and Ammonium Aqueous *Frontiers in Chemistry* **8** 1–11.
[32] Cen QG, Fang MX, Xu JP, Luo ZY. 2012 Experimental Study of Breakthrough Adsorption on Activated Carbon for CO2 Capture *Advanced Materials Research* **356-360** 1139-44.
[33] Auta M, Hameed BH. 2014 Adsorption of carbon dioxide by diethanolamine activated alumina beads in a fixed bed *Chem Eng J* **253** 350-5.
[34] Fashi F, Ghaemi A, Moradi P. 2019 Piperazine-modified activated alumina as a novel promising candidate for CO2 capture: experimental and modeling *Greenhouse Gases: Science and Technology* **9**(1) 37-51.
[35] Tan YL, Islam MA, Asif M, Hameed BH. 2014 Adsorption of carbon dioxide by sodium hydroxide-modified granular coconut shell activated carbon in a fixed bed *Energy* **77** 926-31.
[36] Abdul Kareem FA, Shariff AM, Ullah S, Dreisbach F, Keong LK, Mellon N, et al. 2018 Experimental measurements and modeling of supercritical CO2 adsorption on 13X and 5A

zeolites *Journal of Natural Gas Science and Engineering* **50** 115-27.
[37] Azharul Islam M, Tan YL, Atikul Islam M, Romić M, Hameed BH. 2018 Chitosan–bleaching earth clay composite as an efficient adsorbent for carbon dioxide adsorption: Process optimization *Colloids and Surfaces A: Physicochemical and Engineering Aspects* **554** 9-15.
[38] Gómez-Pozuelo G, Sanz-Pérez ES, Arencibia A, Pizarro P, Sanz R, Serrano DP. 2019 CO2 adsorption on amine-functionalized clays *Microporous Mesoporous Mater* **282** 38-47.